vibration

MDPI

Article

Unidirectional Flow Through Time-Dependent Cross-Sectional Areas of a Compliant Tube and a Valve: A Nonlinear Model

Christos Manopoulos [1,*], Sokrates Tsangaris [1], Christina Georgantopoulou [2] and Dimitrios Mathioulakis [2]

[1] Laboratory of Biofluid Mechanics & Biomedical Technology, Fluids Section, School of Mechanical Engineering, National Technical University of Athens, Heroon Polytechniou 9, Zografos, 15780 Athens, Greece; sgt@fluid.mech.ntua.gr

[2] Mechanical Department, School of Engineering, Bahrain Polytechnic, Isa Town P.O. Box 33349, Bahrain; christina@polytechnic.bh (C.G.); dimitrios.mathioulakis@polytechnic.bh (D.M.)

* Correspondence: manopoul@fluid.mech.ntua.gr or manopoul@central.ntua.gr

Abstract: This work investigates the conditions for net flow generation by a straight tube with a cross-sectional area harmonically varying in time that connects two tanks—a problem that is mainly found in the design of impedance pumps. By assuming a quasi-one-dimensional flow and applying continuity and momentum equations, a first-order differential equation with respect to the flow rate is derived and presented for the first time, including a nonlinear term that is responsible for net flow rate generation. Namely, the net flow rate is found to be nonzero (as is the nonlinear term) if the cross-sectional areas of the two tanks are unequal and one of them is smaller than that of the straight tube. In this case, the flow is directed from the smaller to the larger tank and the net flow rate increases with the frequency of the tube's cross-sectional area variation. In contrast, when the tanks' cross-sections are equal, the net flow is generated only if a valve is installed, e.g., at one end of the tube, due to the large asymmetries imposed in the hydraulic losses with respect to the tube mid-length. Compared with constant valve opening, the net flow rate is augmented significantly if the valve opening is time-dependent. By employing the same equation, the flow rate of an intra-aortic counter-pulsating balloon pump is also examined, in which the valve (representing the aortic valve) opens during the shrinkage of the tube, and it is shown that the net flow rate increases with the frequency and amplitude of the tube's cross-sectional area. Conclusively, the harmonic oscillation in time of a tube's wall can cause unidirectional flow only if asymmetric losses are present with respect to its mid-length.

Keywords: impedance pump; net flow rate; nonlinear flow model; time-dependent cross-sectional area; local losses; intra-aortic balloon pump

Citation: Manopoulos, C.; Tsangaris, S.; Georgantopoulou, C.; Mathioulakis, D. Unidirectional Flow Through Time-Dependent Cross-Sectional Areas of a Compliant Tube and a Valve: A Nonlinear Model. *Vibration* **2024**, *7*, 987–998. https://doi.org/10.3390/vibration7040052

Academic Editors: Francesco Pellicano, Yuri Mikhlin, Konstantin V. Avramov and Antonio Zippo

Received: 21 August 2024
Revised: 9 October 2024
Accepted: 18 October 2024
Published: 29 October 2024

1. Introduction

Although the majority of pumps (e.g., centrifugal or axial flow pumps) essentially consist of a number of rotating blades—the kinetic energy of which is transferred to the conveyed fluid—there are also some other types of pumps that add energy to fluids by means of the moving walls of flexible conduits or membranes. In the second category of pumps, there are two main types: peristaltic and impedance pumps. In peristaltic pumps, a flexible tube is pressed by a rotating roller so that a moving stenosis is formed, traveling along the tube. As a result, the cross-sectional area of the tube is a well-defined function of axial distance and time. In contrast, an impedance pump consists mainly of a flexible tube, a part of which is periodically compressed and decompressed by a pincher with a given amplitude and frequency. Especially in micro-scale applications, impedance pumps cause the motion of fluid with a membrane that oscillates over a cavity by an external energy source, e.g., piezoelectric actuators, electromagnetic forcing, etc. [1]. Compared with peristaltic pumps, the net flow rate of impedance pumps is harder to predict since this is mainly affected by the reflection of longitudinal pressure waves at sites of the hydraulic

loop, where there is an abrupt change in the tube's material, like at the connection of a soft tube with a stiff one. As a result, the time-dependent streamwise pressure distribution is quite complex, which, in turn, deforms the tube walls and accordingly influences the pump flow rate. In contrast to peristaltic pumps, in which the flow rate is a linear function of the frequency of the rollers, in impedance pumps, the flow rate is a nonlinear function of the pincher frequency [2]. More specifically, the net flow rate maximizes at various pinching frequencies as a result of a resonance phenomenon, namely, when these frequencies coincide with the natural frequencies of the hydraulic installation. Moreover, it is interesting to note that with the increase in pinching frequency, the sign of the net flow rate also changes, alternating from positive to negative. The above natural frequencies mainly depend on (a) the tube material properties (e.g., Young's modulus, Poisson's ratio, and wall thickness), which affect the speed of the traveling pressure disturbances, and (b) the length of the tube. It is thus the complex interaction between the fluid and the deformable tube wall that makes the problem difficult to solve. The above has been examined in multiple publications in the open literature in the last seventy years, some of which are mentioned here [3–12]. Nevertheless, there are still open questions that need to be answered regarding a more efficient design for this type of pump.

In micro impedance pumps, the whole flexible area moves in a predetermined way over a cavity. In order to increase the net flow rate, taper-type tube segments are normally introduced at the connection of the cavity with the microchannels so that the flow is turned into a unidirectional flow despite the harmonic motion in time of the membrane [13]. Essentially, the taper-tube segments cause an asymmetry to the hydraulic losses with respect to the membrane location so that although the fluid goes back and forth (induced by the membrane motion), its displacement is nonzero during each period. In [14], various configurations of piezoelectric impedance pumps are presented, and in [15], several flow rectifiers applied in micropumps—as active and passive valves—are discussed. In a recent effort by this group, a time-dependent passive valve was introduced in a valveless pump circuit, enhancing the net flow rate several times, especially at small amplitudes of the pump's pincher [16].

Another interesting impedance type of pump used in hemodynamics is the so-called intra-aortic balloon pump, which is a type of mechanical support for the failing heart that was introduced in clinical practice in the 1960s [17]. It consists of a balloon of cylindrical shape inserted into the human descending aorta, which inflates during diastole and deflates during systole, affecting the aortic pressure waveform and the blood flow rate. In other words, the cross-section of the free passage of blood in the descending aorta varies in time, as it is increased during systole and decreased during diastole. The basic parameters involved in this pump are the volume of the balloon and the timing of its inflation–deflation with respect to the aortic valve opening–closing. Numerical flow simulations of this pump, including the arterial system, have been presented in the literature based on lumped flow models with electrical circuit analogies, including resistance, inductance, and capacitance elements [18–20].

In the present numerical work, a quasi-one-dimensional flow model is employed in the study of a pumping system that consists of a straight tube of a predetermined cross-sectional area harmonically varying in time with or without a valve at one of its two ends, of a constant or time-varying opening. The tube is connected to two tanks of arbitrary cross-sections. The aim of this work is the investigation of the conditions for net flow rate generation in impedance pumps. Based on continuity and momentum equations, a first-order nonlinear differential equation of the flow rate is derived, which is presented and solved here for the first time, which is one of the novel features of this work. Most importantly, it is shown that its nonlinear term is responsible for net flow rate generation, being nonzero only if asymmetries in the hydraulic losses exist with respect to the mid-length of the tube. These losses are due to either abrupt changes in the fluid conduit cross-sectional area or, more importantly, the presence of a valve. Practically, the examined hydraulic system resembles an impedance pump in which the tube's walls or a membrane are oscillating in a known, deterministic way, not being affected by the fluid

forces. In other words, the procedure followed does not take into account the case where the shape of the tube changes due to its interaction with the fluid, which occurs in some impedance pumps. Moreover, the case of a valve of a time-dependent opening installed in the system, besides its potential application in impedance pumps, is also examined in the context of an intra-aortic balloon pump for various heart rates and inflated diameters of the balloon, assuming that the valve plays the role of the aortic valve. The findings of this work could be used in the design of impedance pumps and intra-aortic balloon pumps.

2. Materials and Methods

This work numerically examines the flow between two open tanks, 1 and 2, connected by a straight tube of length L, with a cross-sectional area $A(t)$ harmonically varying in time with a cyclic frequency ω, including, in the general case, a time-dependent constriction at the right end of the tube $A_{02}(t)$ (Figure 1).

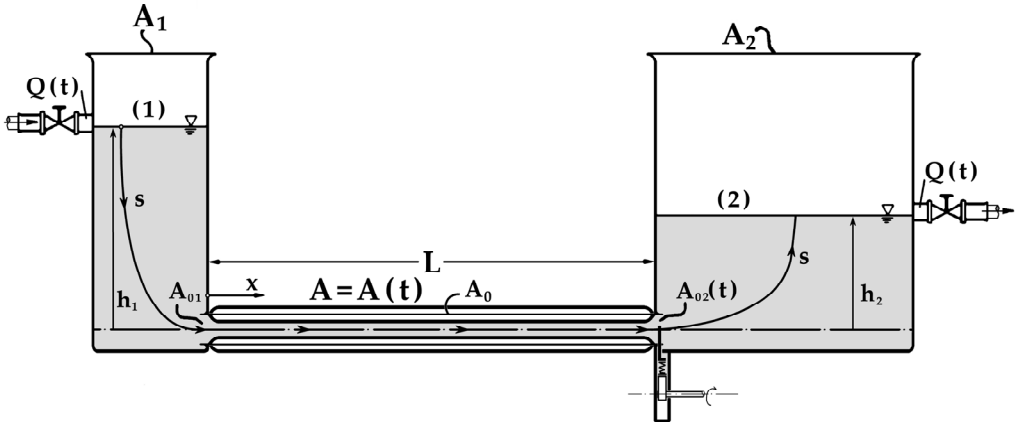

Figure 1. Hydraulic installation.

The cross-sectional areas of the tanks are denoted as A_1 and A_2, and their elevations are h_1 and h_2, respectively. The general expression of the continuity equation is:

$$\frac{\partial \rho}{\partial t} + div(\rho \vec{v}) = 0 \tag{1}$$

where ρ is the fluid density and $\vec{v}$ is the fluid velocity vector. By employing a quasi-one-dimensional flow model (taking into account the radial displacement of the tube wall) and assuming that the flow is incompressible, after some manipulation, the above equation is written as follows:

$$\frac{\partial A}{\partial t} + \frac{\partial (A v_x)}{\partial x} = 0 \tag{2}$$

where v_x is the axial (average in space) fluid velocity in a tube's cross-section.

By assuming that the flow is laminar, the momentum equation along an arbitrary direction s is given by:

$$\rho \frac{\partial v_s}{\partial t} + \frac{\rho}{2} \frac{\partial \left(v_s^2\right)}{\partial s} + \frac{\partial p}{\partial s} + \rho g \frac{dh}{ds} + 8\pi \rho \nu \frac{v_s}{A} = 0 \tag{3}$$

where v_s is the fluid velocity along s, p is the static pressure, h is the elevation, and ν is the fluid's kinematic viscosity. In Equation (3), the fluid inertia is counterbalanced by the pressure, gravity, and viscosity forces. In particular, the last term of (3) is the known viscous term of the Poiseuille flow. More details about the derivation of Equation (3) can be found in [21].

In case a tube's cross-sectional area changes stepwise, like at the junctions of the tube with the tanks, the hydraulic losses depend on the ratio of the two areas and the direction of the flow. Namely, if the flow is directed from a smaller to a larger cross-section ('case 1'), the losses are higher (due to flow separation) than in the opposite direction ('case 2'). Based

mainly on experimental observations, the hydraulic losses are expressed as a function of the dynamic pressure at the smaller cross-sectional area multiplied by a coefficient. The loss coefficient at tank 1's tube junction is designated by the Greek letter 'ξ', whereas, at tank 2's tube junction, it is by the Greek letter 'ζ'. Each of the two coefficients has an index numbered '1' if the flow is from smaller to larger cross-sections and has '2' when the flow is in the opposite direction. Moreover, the expressions of the coefficients depend on whether the flow is directed from the tube to the tank or vice versa. The coefficients ξ_1 and ξ_2 are given by the following expressions (4)–(7) in which the cross-sectional area of tank 1 has been nondimensionalized by the tube time-averaged cross-sectional area A_0, namely $\widetilde{A}_1 = A_1/A_0$ [22]:

(a) If $A_1 > A_0$ and the flow direction is from the tube to tank 1 ('case 1'), the coefficient of the hydraulic losses ξ_1 is:

$$\xi_1 = \left(1 - \frac{1}{\widetilde{A}_1}\right)^2 \tag{4}$$

(b) If $A_1 > A_0$ and the flow direction is from tank 1 to the tube, namely towards a reduced area ('case 2'), the coefficient of the hydraulic losses ξ_2 is:

$$\xi_2 = 0.587 + \frac{0.395}{\sqrt{\widetilde{A}_1}} - \frac{4.538}{\widetilde{A}_1} + \frac{14.243}{\sqrt{\widetilde{A}_1^3}} - \frac{19.222}{\widetilde{A}_1^2} + \frac{8.54}{\sqrt{\widetilde{A}_1^5}} \tag{5}$$

(c) If $A_1 < A_0$ and the flow direction is from tank 1 to the tube ('case 1'), the coefficient of the hydraulic losses ξ_1 is:

$$\xi_1 = (1 - \widetilde{A}_1)^2 \tag{6}$$

(d) If $A_1 < A_0$ and the flow direction is from the tube to tank 1 ('case 2'), the coefficient of the hydraulic losses ξ_2 is:

$$\xi_2 = 0.587 + 0.395\sqrt{\widetilde{A}_1} - 4.538\widetilde{A}_1 + 14.243\sqrt{\widetilde{A}_1^3} - 19.222A_1^2 + 8.54\sqrt{\widetilde{A}_1^5} \tag{7}$$

Similarly, the hydraulic coefficient at the junction of the tube with tank 2, denoted by 'ζ' with an index of 1 or 2, is expressed in the same way as the coefficient ξ, in which $\widetilde{A}_2$ is used instead of $\widetilde{A}_1$.

A spatial integration of the momentum and continuity equations, taking into account the hydraulic losses at the two tank-tube junctions, ends up with the following first-order nonlinear differential equation with respect to the flow rate Q at tank 1's tube junction:

$$B(t)\dot{Q} + C(t)Q + D(t)Q^2 + E(t) = 0 \tag{8}$$

where the coefficients $B(t)$, $C(t)$, $D(t)$, and $E(t)$ are:

$$B(t) = \frac{h_1}{A_1} + \frac{h_2}{A_2} + \frac{L}{A(t)}, \tag{9}$$

$$C(t) = 8\pi\nu\left(\frac{h_1}{A_1^2} + \frac{h_2}{A_2^2} + \frac{L}{[A(t)]^2}\right) - \left(\frac{\pm\zeta_{1,2}}{A_{02}^2} + \frac{1}{A_2^2}\right)\frac{dV(L,t)}{dt} + \frac{\partial}{\partial t}\left(\frac{L}{A(t)}\right), \tag{10}$$

$$D(t) = \frac{1}{2}\left(\frac{1}{A_2^2} - \frac{1}{A_1^2} \pm \frac{\xi_{1,2}}{A_{01}^2} \pm \frac{\zeta_{1,2}}{A_{02}^2}\right), \tag{11}$$

$$\begin{aligned} E(t) = g(h_2 - h_1) - \frac{h_2}{A_2}\frac{d^2V(L,t)}{dt^2} + \frac{1}{2}\left(\frac{\pm\zeta_{1,2}}{A_{02}^2} + \frac{1}{A_2^2}\right)\left[\frac{dV(L,t)}{dt}\right]^2 - 8\pi\nu\frac{h_2}{A_2^2}\frac{dV(L,t)}{dt} \\ - \frac{L}{A(t)}\frac{d^2V(L,t)}{dt^2} - \frac{\partial}{\partial t}\left(\frac{L}{A(t)}\right)\frac{dV(L,t)}{dt} - 8\pi\nu\frac{L}{[A(t)]^2}\frac{dV(L,t)}{dt}, \end{aligned} \tag{12}$$

In the above expressions, A_{01} and A_{02} refer to the cross-sectional areas at the tube-tank junctions, and $V(L,t)$ is the time-dependent volume of the tube. In the expressions (10) to (12), the positive sign in the coefficients ξ_i and ζ_i is used when the flow direction is from tank 1 to tank 2. Briefly, Equation (8) was derived according to the following procedure: a spatial integration of the momentum Equation (3) was applied in three cases, namely between the free surface of tank 1 and its junction

with the tube, between the free surface of tank 2 and its junction at the other end of the tube, and finally, between the two ends of the tube. Moreover, based on spatial integration of the continuity equation, an expression of the fluid speed along the tube was derived, which is a function of the tube's cross-sectional area and the flow rate at one end of the tube. More details regarding the derivation of the above expressions are in [23].

In order to generalize the results, the following non-dimensional numbers are used,

$$\widetilde{t} = t\omega,\ \widetilde{A}_i = A_i/A_0,\ \widetilde{Q} = Q/(A_0\omega L)\ and\ W = R_0\sqrt{\omega/\nu}, \tag{13}$$

where A_i refers to A_{01}, A_{02}, and A_b; R_0 is the tube's internal radius corresponding to the tube's undeformed cross-sectional area A_0; and ω is the cyclic frequency of the tube's oscillating area A varying with an amplitude A_b, namely

$$\widetilde{A} = 1 + \widetilde{A}_b cos\widetilde{t} \tag{14}$$

The non-dimensional number W in (13) is the known Womersley number. If the tank elevations are $h_1 = h_2 = 0$, the coefficients $B(t)$ to $E(t)$ are simplified and are given in non-dimensional form in (15), in which $V(L,t)$ being the total tube internal volume has been replaced by the product $A(t)\cdot L$:

$$\widetilde{B}(\widetilde{t}) = \frac{1}{\widetilde{A}},$$

$$\widetilde{C}(\widetilde{t}) = \frac{8}{W^2}\frac{1}{\widetilde{A}^2} - \left(\frac{\pm\zeta_{1,2}}{\widetilde{A}_{02}^2} + \frac{1}{\widetilde{A}_2^2} + \frac{1}{\widetilde{A}^2}\right)\frac{d\widetilde{A}}{d\widetilde{t}},$$

$$\widetilde{D}(\widetilde{t}) = \frac{1}{2}\left(\frac{1}{\widetilde{A}_2^2} - \frac{1}{\widetilde{A}_1^2} \pm \frac{\xi_{1,2}}{\widetilde{A}_{01}^2} \pm \frac{\zeta_{1,2}}{\widetilde{A}_{02}^2}\right),$$

$$\widetilde{E}(\widetilde{t}) = -\frac{1}{2\widetilde{A}}\frac{d^2\widetilde{A}}{d\widetilde{t}^2} + \frac{1}{2}\left(\frac{\pm\zeta_{1,2}}{\widetilde{A}_{02}^2} + \frac{1}{\widetilde{A}_2^2} + \frac{1}{\widetilde{A}^2}\right)\left(\frac{d\widetilde{A}}{d\widetilde{t}}\right)^2 - \frac{8}{W^2}\frac{1}{2\widetilde{A}^2}\frac{d\widetilde{A}}{d\widetilde{t}}, \tag{15}$$

The nonlinear differential Equation (8), in its non-dimensional form, is solved numerically with respect to $\widetilde{Q}$ by using a Runge–Kutta of fourth order, as it is explained in Appendix A, with a non-dimensional time interval of 10^{-3} to secure a small truncation error (of the order of 10^{-12}). It has to be noted that due to the complex coefficients of Equation (8), which is the known Riccati differential equation, no analytical solution is available. By knowing $\widetilde{Q}(\widetilde{t})$, the net flow rate was calculated based on three periods of oscillation after the solution reached a steady state. Since the hydraulic loss coefficients at the tank-tube junctions $\xi_{1,2}$ and $\zeta_{1,2}$ take relatively low values, namely between 0 and 1, it was decided to include a gate valve in the hydraulic circuit, installed at the tank 2-tube junction, aiming to enhance the asymmetries in the hydraulic installation by increasing the flow resistance at one of the tube ends. Moreover, by including the gate valve, it was also possible to simulate the operation of an intra-aortic balloon pump by assuming that the valve plays the role of the aortic valve. According to Figure 2, the loss coefficient ζ of a gate valve takes a value as high as 400 when its opening h is 6.6% of the tube diameter d or 8.4% of the tube cross-sectional area [24].

Due to the induced flow asymmetries, the gate valve can further increase the net flow rate, as it is shown below in the Section 3. In order to estimate the valve's hydraulic losses, the spatially average fluid velocity at the gate opening is calculated based on the local flow rate and its area A_{02}, which is given by:

$$A_{02} = \left[\pi - 2\left(cos^{-1}\mu - \mu\sqrt{1-\mu^2}\right)\right]\frac{d^2}{4},\ \ 0 < \mu < 1 \tag{16}$$

where $\mu = h/d$ (see Figure 2). The derivation of (16) was based on simple geometrical formulas by computing the area between two equal circles (note that the gate valve seat area equals the pipe area) of diameter d, the centers of which are at a distance h apart (see Figure 2).

Another option was also examined, namely when the gate valve opening varies in time, which could be used in an impedance pump to control its flow rate or to simulate the opening–closing of the aortic valve in the study of an intra-aortic balloon pump. In this case, the following expression of A_{02} was arbitrarily used:

$$\widetilde{A}_{02} = \widetilde{A}_{02,min} + \left(1 - \widetilde{A}_{02,min}\right)cos^{40}\left[sin^4(\widetilde{t}/2)\right], \tag{17}$$

where $\widetilde{A}_{02,min}$ is the minimum dimensionless area of the gate valve opening. Expression (17) was devised based on the fact that the aortic valve opens and closes in an almost stepwise manner. By knowing the area A_{02} at each time instant from Equation (17), the ratio μ was calculated from (16), and consequently, the hydraulic loss coefficient ζ of the valve was determined from the graph of Figure 2.

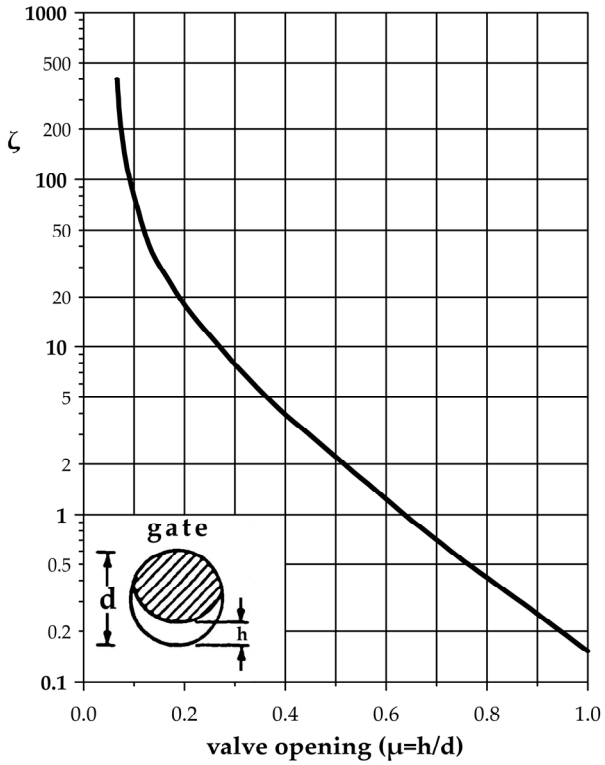

Figure 2. Gate valve loss coefficient [24] (p. 273).

In the next paragraph, the net flow rate is examined in the following three cases: (a) Two tanks at zero height are connected by a straight horizontal tube of uniformly oscillating walls, with no valve present. In this case, the net flow rate is calculated for various ratios of the tanks' cross-sectional areas $\widetilde{A}_1/\widetilde{A}_2$ for a certain Womersley number, as well as for a range of Womersley numbers and given ratios $\widetilde{A}_1/\widetilde{A}_2$. (b) Aside from the oscillating tube, the influence of a gate valve is also studied, where it is installed at tube one's end, the opening of which is either constant or time-dependent. The time-dependent opening of the valve is shown to be far more efficient in net flow rate generation compared with the constant opening. (c) The flow rate of an intra-aortic balloon pump is examined for various heart rates and balloon-inflated diameters (by varying the A_b parameter), considering that the valve plays the role of a leaky aortic valve.

3. Results and Discussion

3.1. No Valve Is Used

If the gate valve is absent and the two tanks have equal cross-sectional areas ($A_1 = A_2$), the coefficient $D(t)$ of the nonlinear term of Equation (8) becomes zero, as well as the net flow rate. Since the tube area varies harmonically in time and there are no flow asymmetries with respect to the mid-length of the tube, the fluid moves back and forth without being transferred from one tank to the other. However, when A_1 differs from A_2, the hydraulic loss coefficients $\xi_{1,2}$ and $\zeta_{1,2}$ are different, inducing flow asymmetries so that the flow becomes, on average, unidirectional, directed from the smaller to the larger tank. Figure 3 shows the net flow rate as a function of the ratio of the cross-sectional areas of the tanks $\widetilde{A}_1/\widetilde{A}_2$ for various values of $\widetilde{A}_2$, by keeping constant the frequency of the tube oscillation ($W = 5$) with a 10% tube area amplitude ($\widetilde{A}_b = 0.1$). It is known that for small W values (e.g., $W < 1$), the flow in a tube is quasi-steady. However, by progressively increasing W, the unsteadiness of the flow becomes dominant, changing the parabolic velocity profile to a flatter one [25]. In the present case, the spatial change in the velocity in each cross-section is not taken into account since the flow is assumed to be one-dimensional, and a spatially average velocity is considered in each tube cross-section.

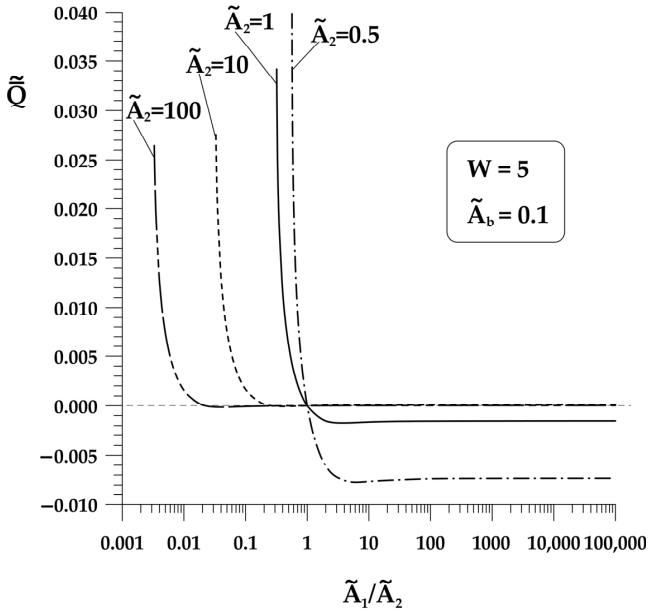

Figure 3. Net flow rate versus tank cross-sectional areas. $W = 5$, $\widetilde{A}_b = 0.1$.

All curves in Figure 3 go through the point $\widetilde{A}_1/\widetilde{A}_2 = 1$ and zero net flow rate, which is the case of no flow asymmetries in the system. In contrast, the net flow rate increases exponentially when one of the two tanks' cross-sectional areas takes smaller values than that of the tube; for example, in the case $A_1 = 0.326\ A_0$ for which the non-dimensional net flow rate takes a value of 0.028 (see Figure 3, $\widetilde{A}_2 = 1$ and $\widetilde{A}_1/\widetilde{A}_2 = 0.326$). However, when both tanks have larger cross-sections than that of the tube, the net flow rate is again zero. This finding could be applied to impedance micro pumps, in which the size of the cavity where the membrane oscillates has to be larger than at least one of the micro-tubes that is connected to the cavity.

When the frequency of the tube walls' oscillation increases, the net flow rate also increases. Figure 4 shows the variations in the net flow rate with the Womersley number when one or both tanks have smaller cross-sections than the tube's cross-section. Moreover, the net flow rate takes nonzero values when the Womersley number exceeds 0.5, and it increases exponentially for $W > 5$. Since W is inversely proportionate to the square root of the fluid kinematic viscosity, the net flow rate of water will be higher than that of blood and much higher than of air. The opposite signs of the two curves of Figure 4 denote opposite flow directions, with the positive to be directed from tank 1 to tank 2. Therefore, like in Figure 3, the flow is directed from the smaller to the larger tank.

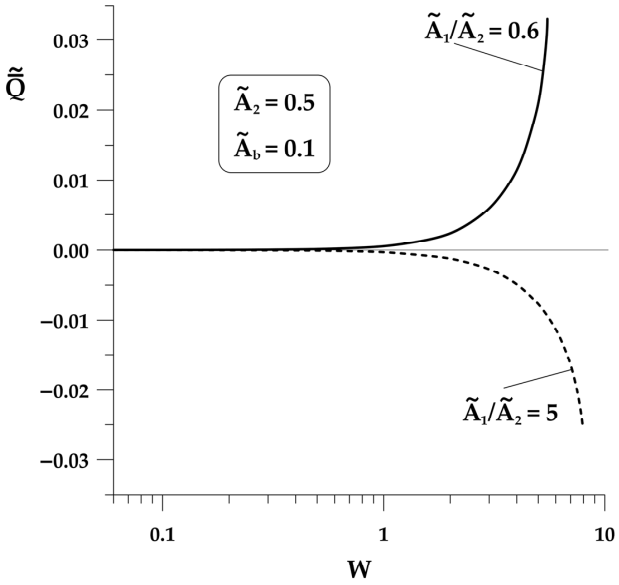

Figure 4. Net flow rate versus Womersley number.

3.2. A Gate Valve Is Used

3.2.1. Constant Valve Opening

When the gate valve is introduced at the connection of the tube with tank 2, the pumping effect of the oscillating tube is enhanced, so if the tanks have equal cross-sectional areas, a net flow rate is established. As it is shown in Figure 5 for equal tanks, $\widetilde{A}_b = 0.1$ and $W = 5$, the flow is directed towards tank 2 and maximizes when the gate valve loss coefficient is $\zeta = 6.5$, corresponding to a valve opening of 37.6% of the mean tube cross-section. Consequently, in an impedance pump, the use of a valve in the hydraulic system could boost the net flow rate when the opening of the valve is suitable. In practice, instead of valves, taper tubes are used as flow rectifiers, with hydraulic losses strongly dependent on their geometry (width-taper angle) and Reynolds number. According to [26], the performance of such devices drops or even vanishes at *Re* below 50, which seems to be remedied by using taper tubes with flexible covers so that, in this case, they work efficiently, even for $Re < 10$ [27].

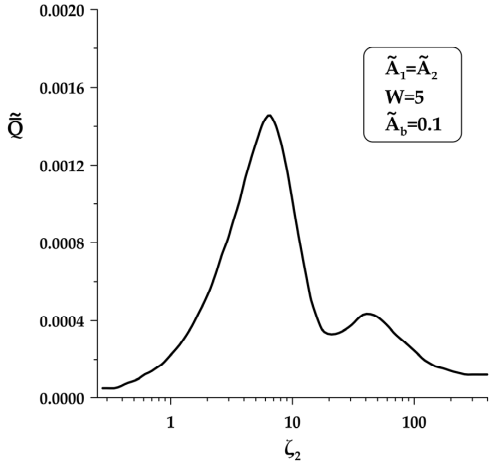

Figure 5. Net flow rate versus valve loss coefficient. Valve opening constant.

3.2.2. Time-Dependent Valve Opening

In this paragraph, the opening of the valve is considered time-dependent. The valve can be part of the hydraulic loop of an impedance pump as a means to control its flow rate, or in the case of an intra-aortic balloon pump, it can simulate the operation of an aortic valve. Among several scenarios regarding the timing between the valve opening and the tube cross-sectional area variation, the case of the balloon pump was followed. Namely, the opening of the valve coincides with an increase in the tube cross-sectional area since, at the same time, the balloon shrinks. Figure 6 shows the variations in the tube cross-sectional area $\widetilde{A}(\tilde{t})$ along with that of the valve opening $\widetilde{A}_{02}$, following Equation (17), with $A_{02,min}$ being equal to 8.4 % of A_0 (corresponding to $\zeta \approx 400$) and $\widetilde{A}_b = 0.1$.

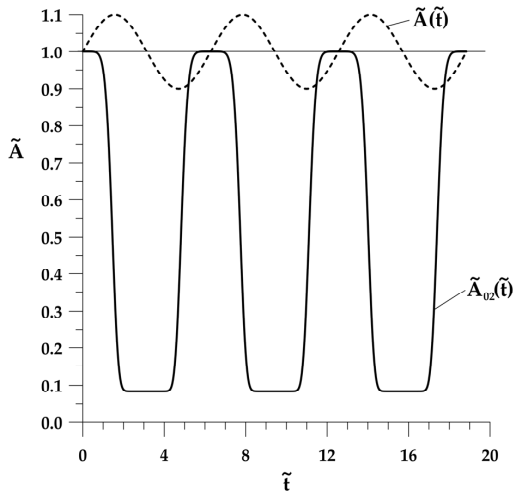

Figure 6. Tube (dashed line) and gate valve (continuous line) cross-sectional areas versus non-dimensional time. $\widetilde{A}_{02,min} = 0.084$.

By varying the minimum area of the valve and keeping the frequency of the tube and valve oscillation constant (W = 5), the graph in Figure 7 was obtained for equal tank cross-sections. It is clear from Figure 7 that the net flow rate is about 10 times larger compared to the case where the valve opening is constant, and the maximum value of the net flow rate occurs for $\widetilde{A}_{02,min} = 25.3\%$. Moreover, it is interesting to note that the maximization of the net flow rate does not require that the valve closes completely. A similar phenomenon is detected in [16], in which an unsteady stenosis increased the net flow rate by 19 times.

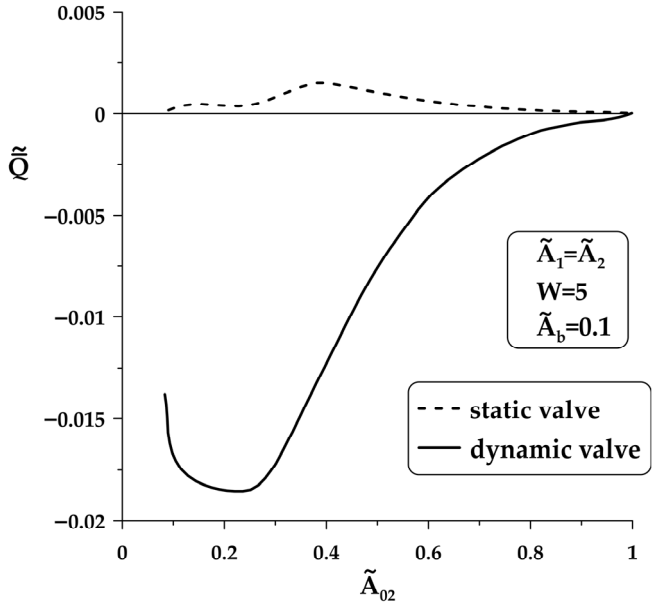

Figure 7. Net flow rate versus valve minimum cross-sectional area. Static and dynamic cases.

By increasing the frequency of the straight tube pulsation and its cross-sectional area amplitude $\widetilde{A}_b$, the non-dimensional net flow rate increases up to a Womersley value of 5 and then it remains constant (see Figure 8). The fact that the non-dimensional net flow rate is independent of W when W takes high values is attributed to the W^{-2} terms in Equation (8), which tend toward zero when W goes to infinity. Therefore, the net flow rate $\overline{Q}$ at high frequencies increases linearly with the frequency, according to the definition of the non-dimensional flow rate $\widetilde{Q} = Q/(A_0\omega L)$, namely, $\overline{Q} = A_0\omega L\widetilde{\overline{Q}}$.

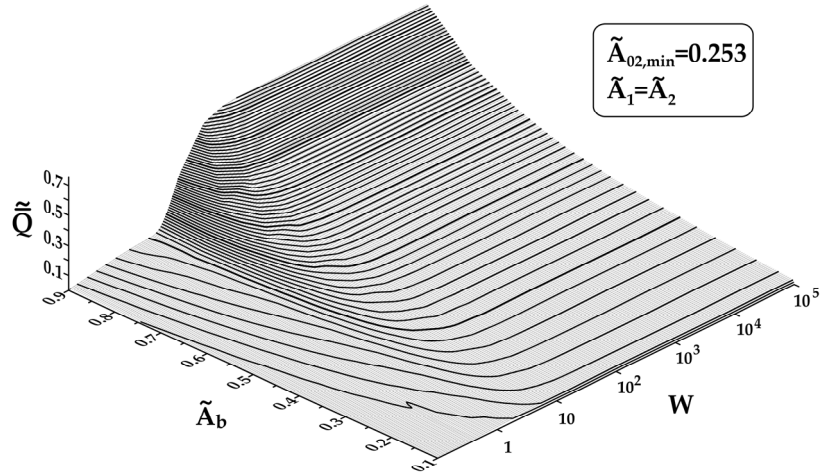

Figure 8. Dimensionless net flow rate versus $\widetilde{A}_b$ and W.

3.2.3. Intra-Aortic Balloon Pump

For the case of the aortic balloon pump, the following assumptions were made: blood is the flowing medium of hematocrit 40 so that its kinematic viscosity is 4.0072 cSt [28]; the heart rate varies from 70 to 120 beats/min, or the cyclic frequency ω changes from 7.3 up to 12.5 rad/s; the aorta internal diameter is 20 mm; the two tanks have the same diameter as that of the aorta; the length of

the balloon is 0.26 m, based on [29]; A_b varies from 6 to 24.5% of A_0; and the minimum opening of the valve is 8.4% of A_0. It should be noted that in balloon pumps, the inflated balloon's diameter normally does not exceed 80% of the descending thoracic aorta diameter [30], or the A_b maximum value is close to 30% of A_0. Moreover, the present model simulates cases of leaky aortic valve leaflets, where the area of the valve that remains open, according to [31], is 25% of the cross-sectional area of the left ventricular outflow tract (for mild cases).

Figure 9 shows the net flow rate iso-contours as a function of both the inflation of the balloon—which is related to A_b—and the heart rate. According to Figure 9, the generated net flow rate takes a maximum value close to 1 L/min for a frequency of 2 Hz and A_b = 24% of A_0. Nevertheless, it has to be remembered that in real applications, the arterial tree plays a significant role in the pump's performance, such as its compliance, which has been shown to reduce the balloon efficiency when this increases [32]. Of course, the procedure, although relatively simplistic, is able to reproduce the basic features of the pump.

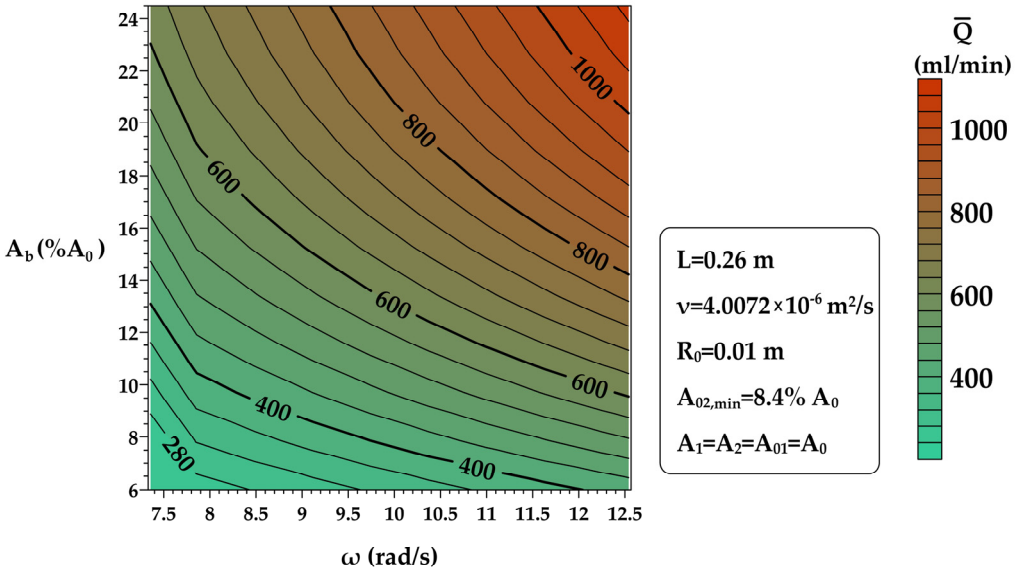

Figure 9. Net flow rate versus frequency and tube oscillation amplitude.

4. Conclusions

This work numerically examines, by employing a quasi-one-dimensional flow model, the conditions for which the net flow rate is generated by the harmonic variations in time of the cross-sectional area of a tube connecting two tanks. A first-order nonlinear differential equation of the flow rate was derived, showing that its nonlinear term is responsible for the net flow rate generation, being associated with asymmetries in the hydraulic losses with respect to the mid-length of the tube. The net flow rate is nonzero if the tank cross-sectional areas are not equal; it takes higher values if at least one of the tanks has a smaller area than that of the tube, is directed from the smaller to the larger tank, and increases with the frequency of the tube oscillation. When the tanks' cross-sections are equal, the net flow is null. In this case, if a valve is installed, the flow becomes unidirectional, and it is further increased if the valve opening is time-dependent, maximizing for a particular minimum valve opening. By simulating the operation of an intra-aortic balloon pump so that the valve opening coincides with the shrinkage of the tube, the net flow rate increases with the heart rate and the inflation of the balloon.

Author Contributions: Conceptualization, S.T. and C.M.; methodology, S.T. and C.M.; software, C.M.; validation, C.M.; formal analysis, C.M.; investigation, C.M. and D.M.; resources, C.M., C.G. and D.M.; data curation, C.M.; writing—original draft preparation, C.M. and D.M.; writing—review and editing, C.M., S.T., C.G. and D.M.; visualization, C.M.; supervision, S.T.; project administration, C.M. All authors have read and agreed to the published version of the manuscript.

Funding: This research received no funding.

Data Availability Statement: Data are contained within the article.

Conflicts of Interest: The authors declare no conflicts of interest.

Appendix A

Numerical Method for Solving the Nonlinear Ordinary Differential Equation

To solve the ordinary differential Equation (8), a FORTRAN program implementing the classical fourth-order Runge–Kutta method is used as a single-step time marching scheme. In this method, the time derivative of the unknown dimensionless flow rate function is isolated as follows:

$$\frac{d\widetilde{Q}}{d\widetilde{t}} = \dot{\widetilde{Q}} = -\frac{\widetilde{C}(\widetilde{t})\cdot\widetilde{Q} + \widetilde{D}(\widetilde{t})\cdot\widetilde{Q}^2 + \widetilde{E}(\widetilde{t})}{\widetilde{B}(\widetilde{t})} \tag{A1}$$

Next, the following coefficients of each order are calculated for each dimensionless time interval $\Delta\widetilde{t}$ [33].

$$k_1 = \dot{\widetilde{Q}}(\widetilde{t}_i, \widetilde{Q}_i) = -\frac{\widetilde{C}(\widetilde{t}_i)\cdot\widetilde{Q}_i + \widetilde{D}(\widetilde{t}_i)\cdot\widetilde{Q}_i^2 + \widetilde{E}(\widetilde{t}_i)}{\widetilde{B}(\widetilde{t}_i)} \tag{A2}$$

$$\begin{aligned} k_2 &= \dot{\widetilde{Q}}\left(\widetilde{t}_i + \Delta\widetilde{t}/2, \widetilde{Q}_i + \Delta\widetilde{t}\cdot k_1/2\right) \\ &= -\frac{\widetilde{C}(\widetilde{t}_i + \Delta\widetilde{t}/2)\cdot\left(\widetilde{Q}_i + \Delta\widetilde{t}\cdot k_1/2\right) + \widetilde{D}(\widetilde{t}_i + \Delta\widetilde{t}/2)\cdot\left(\widetilde{Q}_i + \Delta\widetilde{t}\cdot k_1/2\right)^2 + \widetilde{E}(\widetilde{t}_i + \Delta\widetilde{t}/2)}{\widetilde{B}(\widetilde{t}_i + \Delta\widetilde{t}/2)} \end{aligned} \tag{A3}$$

$$\begin{aligned} k_3 &= \dot{\widetilde{Q}}\left(\widetilde{t}_i + \Delta\widetilde{t}/2, \widetilde{Q}_i + \Delta\widetilde{t}\cdot k_2/2\right) \\ &= -\frac{\widetilde{C}(\widetilde{t}_i + \Delta\widetilde{t}/2)\cdot\left(\widetilde{Q}_i + \Delta\widetilde{t}\cdot k_2/2\right) + \widetilde{D}(\widetilde{t}_i + \Delta\widetilde{t}/2)\cdot\left(\widetilde{Q}_i + \Delta\widetilde{t}\cdot k_2/2\right)^2 + \widetilde{E}(\widetilde{t}_i + \Delta\widetilde{t}/2)}{\widetilde{B}(\widetilde{t}_i + \Delta\widetilde{t}/2)} \end{aligned} \tag{A4}$$

$$\begin{aligned} k_4 &= \dot{\widetilde{Q}}\left(\widetilde{t}_i + \Delta\widetilde{t}, \widetilde{Q}_i + \Delta\widetilde{t}\cdot k_3\right) \\ &= -\frac{\widetilde{C}(\widetilde{t}_i + \Delta\widetilde{t})\cdot\left(\widetilde{Q}_i + \Delta\widetilde{t}\cdot k_3\right) + \widetilde{D}(\widetilde{t}_i + \Delta\widetilde{t})\cdot\left(\widetilde{Q}_i + \Delta\widetilde{t}\cdot k_3\right)^2 + \widetilde{E}(\widetilde{t}_i + \Delta\widetilde{t})}{\widetilde{B}(\widetilde{t}_i + \Delta\widetilde{t})} \end{aligned} \tag{A5}$$

Each of the k_i values above represents the time slope of the unknown function $\widetilde{Q}$ at dimensionless time $\widetilde{t}$.

Finally, the next value of $\widetilde{Q}$ in the time sequence is found using the following Equation (A6), which represents a weighted average of the k_i slopes:

$$\begin{aligned} \frac{\widetilde{Q}_{i+1} - \widetilde{Q}_i}{\Delta\widetilde{t}} &= \frac{1}{6}(k_1 + 2k_2 + 2k_3 + k_4) \rightarrow \\ \widetilde{Q}_{i+1} &= \widetilde{Q}_i + \left[\frac{1}{6}(k_1 + 2k_2 + 2k_3 + k_4)\right]\cdot\Delta\widetilde{t} \end{aligned} \tag{A6}$$

References

1. Wang, Y.-N.; Fu, L.-M. Micropumps and Biomedical Applications—A Review. *Microelectron. Eng.* **2018**, *195*, 121–138. [CrossRef]
2. Manopoulos, C.G.; Mathioulakis, D.S.; Tsangaris, S.G. One-Dimensional Model of Valveless Pumping in a Closed Loop and a Numerical Solution. *Phys. Fluids* **2006**, *18*, 017106. [CrossRef]
3. Thomann, H. A Simple Pumping Mechanism in a Valveless Tube. *Z. Für Angew. Math. Phys. ZAMP* **1978**, *29*, 169–177. [CrossRef]
4. Jung, E.; Peskin, C.S. Two-Dimensional Simulations of Valveless Pumping Using the Immersed Boundary Method. *SIAM J. Sci. Comput.* **2001**, *23*, 19–45. [CrossRef]
5. Ottesen, J.T. Valveless Pumping in a Fluid-Filled Closed Elastic Tube-System: One-Dimensional Theory with Experimental Validation. *J. Math. Biol.* **2003**, *46*, 309–332. [CrossRef]
6. Hickerson, A.I.; Rinderknecht, D.; Gharib, M. Experimental Study of the Behavior of a Valveless Impedance Pump. *Exp. Fluids* **2005**, *38*, 534–540. [CrossRef]
7. Avrahami, I.; Gharib, M. Computational Studies of Resonance Wave Pumping in Compliant Tubes. *J. Fluid Mech.* **2008**, *608*, 139–160. [CrossRef]
8. Timmermann, S.; Ottesen, J.T. Novel Characteristics of Valveless Pumping. *Phys. Fluids* **2009**, *21*, 053601. [CrossRef]
9. Shin, S.J.; Chang, C.B.; Sung, H.J. Simulation of a Valveless Pump with an Elastic Tube. *Int. J. Heat Fluid Flow* **2012**, *38*, 13–23. [CrossRef]
10. Lee, W.; Lim, S.; Jung, E. Dynamical Motion Driven by Periodic Forcing on an Open Elastic Tube in Fluid. *Commun. Comput. Phys.* **2012**, *12*, 494–514. [CrossRef]
11. Kozlovsky, P.; Rosenfeld, M.; Jaffa, A.J.; Elad, D. Dimensionless Analysis of Valveless Pumping in a Thick-Wall Elastic Tube: Application to the Tubular Embryonic Heart. *J. Biomech.* **2015**, *48*, 1652–1661. [CrossRef] [PubMed]
12. Loumes, L.; Avrahami, I.; Gharib, M. Resonant Pumping in a Multilayer Impedance Pump. *Phys. Fluids* **2008**, *20*, 023103. [CrossRef]

13. Yan, Q.; Yin, Y.; Sun, W.; Fu, J. Advances in Valveless Piezoelectric Pumps. *Appl. Sci.* **2021**, *11*, 7061. [CrossRef]
14. Hou, Y.; He, L.; Hu, D.; Zhang, L.; Yu, B.; Cheng, G. Recent Trends in Structures and Applications of Valveless Piezoelectric Pump—A Review. *J. Micromech. Microeng.* **2022**, *32*, 053002. [CrossRef]
15. Laser, D.J.; Santiago, J.G. A Review of Micropumps. *J. Micromech. Microeng.* **2004**, *14*, R35–R64. [CrossRef]
16. Manopoulos, C.; Mathioulakis, D. Valveless Pumping with an Unsteady Stenosis in an Open Tank Configuration. *Fluids* **2024**, *9*, 141. [CrossRef]
17. Parissis, H.; Graham, V.; Lampridis, S.; Lau, M.; Hooks, G.; Mhandu, P.C. IABP: History-Evolution-Pathophysiology-Indications: What We Need to Know. *J. Cardiothorac. Surg.* **2016**, *11*, 122. [CrossRef]
18. Abdolrazaghi, M.; Navidbakhsh, M.; Hassani, K. Mathematical Modelling of Intra-Aortic Balloon Pump. *Comput. Methods Biomech. Biomed. Engin.* **2010**, *13*, 567–576. [CrossRef]
19. Ferrari, G.; Khir, A.W.; Fresiello, L.; Di Molfetta, A.; Kozarski, M. Hybrid Model Analysis of Intra-Aortic Balloon Pump Performance as a Function of Ventricular and Circulatory Parameters. *Artif. Organs* **2011**, *35*, 902–911. [CrossRef]
20. De Lazzari, C.; De Lazzari, B.; Iacovoni, A.; Marconi, S.; Papa, S.; Capoccia, M.; Badagliacca, R.; Vizza, C.D. Intra-Aortic Balloon Counterpulsation Timing: A New Numerical Model for Programming and Training in the Clinical Environment. *Comput. Methods Programs Biomed.* **2020**, *194*, 105537. [CrossRef]
21. Schaaf, B.W.; Abbrecht, P.H. Digital Computer Simulation of Human Systemic Arterial Pulse Wave Transmission: A Nonlinear Model. *J. Biomech.* **1972**, *5*, 345–364. [CrossRef] [PubMed]
22. Benedict, R.P.; Carlucci, N.A.; Swetz, S.D. Flow Losses in Abrupt Enlargements and Contractions. *J. Eng. Power* **1966**, *88*, 73–81. [CrossRef]
23. Manopoulos, C. Experimental and Theoretical Determination of "Peristaltic Blood Pumps". Master's Thesis, National Technical University of Athens, Athens, Greece, 1999. Available online: https://dspace.lib.ntua.gr/xmlui/handle/123456789/49369?locale-attribute=en (accessed on 1 November 2019).
24. Miller, D.S. *Internal Flow Systems*; BHRA fluid engineering series; BHRA Fluid Engineering: Cranfield, UK, 1978.
25. Zamir, M. *The Physics of Coronary Blood Flow*; Biological and medical physics, biomedical engineering; Springer: New York, NY, USA, 2005.
26. Tao, R.; Ng, T.; Su, Y.; Li, Z. A Microfluidic Rectifier for Newtonian Fluids Using Asymmetric Converging–Diverging Microchannels. *Phys. Fluids* **2020**, *32*, 052010. [CrossRef]
27. Mehboudi, A.; Yeom, J. A Passive Stokes Flow Rectifier for Newtonian Fluids. *Sci. Rep.* **2021**, *11*, 10182. [CrossRef] [PubMed]
28. Hall, J.E.; Hall, J.E.; Guyton, A.C. *Guyton and Hall Textbook of Medical Physiology*, 12th ed.; Saunders: Philadelphia, PA, USA; Elsevier: Philadelphia, PA, USA, 2011.
29. Parissis, H.; Soo, A.; Leotsinidis, M.; Dougenis, D. A Statistical Model That Predicts the Length from the Left Subclavian Artery to the Celiac Axis; towards Accurate Intra-Aortic Balloon Sizing. *J. Cardiothorac. Surg.* **2011**, *6*, 95. [CrossRef] [PubMed]
30. Krishna, M.; Zacharowski, K. Principles of Intra-Aortic Balloon Pump Counterpulsation. *Contin. Educ. Anaesth. Crit. Care Pain* **2009**, *9*, 24–28. [CrossRef]
31. Zoghbi, W. Recommendations for Evaluation of the Severity of Native Valvular Regurgitation with Two-Dimensional and Doppler Echocardiography. *J. Am. Soc. Echocardiogr.* **2003**, *16*, 777–802. [CrossRef]
32. Papaioannou, T.G.; Mathioulakis, D.S.; Nanas, J.N.; Tsangaris, S.G.; Stamatelopoulos, S.F.; Moulopoulos, S.D. Arterial Compliance Is a Main Variable Determining the Effectiveness of Intra-Aortic Balloon Counterpulsation: Quantitative Data from an in Vitro Study. *Med. Eng. Phys.* **2002**, *24*, 279–284. [CrossRef]
33. Chapra, S.C.; Canale, R.P. *Numerical Methods for Engineers*, 7th ed.; McGraw-Hill Education: New York, NY, USA, 2015.